International Journal of Minerals, Metallurgy and Materials
Volume 23, Number 4, April 2016, Page 408
DOI: 10.1007/s12613-016-1250-z

Variation and optimization of acid-dissolved aluminum content in stainless steel

Le-chen Zhang[1,2], *Yan-ping Bao*[1,2], *Min Wang*[1,2], *and Chao-jie Zhang*[1,2]

1) State Key Laboratory of Advanced Metallurgy, University of Science and Technology Beijing, Beijing 100083, China
2) School of Metallurgical and Ecological Engineering, University of Science and Technology Beijing, Beijing 100083, China
(Received: 15 June 2015; revised: 9 October 2015; accepted: 12 October 2015)

Abstract: As a key step in secondary refining, the deoxidation process in clean stainless steel production is widely researched by many scholars. In this study, vacuum oxygen decarburization (VOD) deoxidation refining in a 40-t electric arc furnace + VOD + ingot casting process was analyzed and optimized on the basis of Al deoxidation of stainless steel and thermodynamic equilibrium reactions between the slag and steel. Under good stirring conditions in VOD, the deoxidation reaction reaches equilibrium rapidly, and the oxygen activity in the bulk steel is controlled by the slag composition and Al content. A basicity of 3–5 and an Al content greater than 0.015wt% in the melt resulted in an oxygen content less than 0.0006wt%. In addition, the dissolved oxygen content decreased slightly when the Al content in the steel was greater than 0.02wt%. Because of the equilibrium of the Si–O reaction between the slag and steel, the activity of SiO_2 will increase while the Si content increases; thus, the Si content should be lowered to enable the formation of a high-basicity slag. A high-basicity, low-Al_2O_3 slag and an increased Si content will reduce the Al consumption caused by SiO_2 reduction.

Keywords: martensitic stainless steel; aluminum content; thermodynamic equilibrium; refining; optimization

1. Introduction

Martensitic stainless steel 2Cr13 is a common product because of its low content of noble metals and correspondingly low cost. Due to the high hardenability, fine mechanical properties, and moderate corrosion resistance of martensitic stainless steels, they are widely used in the manufacturing industry to produce components, plastic molds, and surgery tools [1−2]. Therefore, specifications related to cleanliness and the presence of inclusions have been set to satisfy mechanical properties and surface qualities required for such products.

The process commonly used to produce stainless steel from scrap is electric arc furnace + vacuum oxygen decarburization (EAF + VOD). An EAF is used to melt scrap and alloys and remove carbon from steel, and VOD is subsequently used to decarburize and refine the product. A deoxidizer is added during the refining process to reduce Cr–Ni oxides, dissolved oxygen produced by decarburization in the liquid steel, and Fe–Mn oxides in the slag. Deoxidation inclusions are modified by the addition of Ca in a ladle; the inclusions are subsequently absorbed by the slag with the aid of argon stirring. This refining process reduces the total oxygen content and improves the cleanliness of the stainless steel. Scholars have continuously studied methods of controlling deoxidation and inclusions in stainless steel. Ohta and Suito [3] studied the Al–O equilibrium based on $CaO–Al_2O_3$ slag in Fe–Ni and Fe–Cr alloys at 1873 K and determined the values for interaction coefficient between Al and Ni ($e^{Ni}_{Al(Fe)}$) and between Al and Cr ($e^{Cr}_{Al(Fe)}$). Todoroki and Mizuno [4] investigated the effect of SiO_2 in the slag on inclusion compositions in 304 stainless steel with Al deoxidation. The mechanism of inclusion formation, particularly spinel formation, in stainless steels has been investigated [5–8]. Most of these previous studies focused on thermodynamics and control of spinel inclusions in stainless steels. However, the deoxidation mechanism and its industrial application in stainless steel production have rarely been in-

Corresponding author: Yan-ping Bao E-mail: baoyp@ustb.edu.cn

vestigated.

According to the deoxidation mechanism and reaction equilibrium among steels, inclusions, and slag, deoxidation includes both steel deoxidation and slag deoxidation. Al, which is highly reducible, is added to the melt to decrease the dissolved oxygen content, which results in the formation of pure Al_2O_3 or Al_2O_3-containing inclusions. Therefore, the activity of Al_2O_3 can be considered as unity, and inclusions will equilibrate with steel. Some scholars have studied steel deoxidation [9–11], and the precise control of inclusion composition is known to be related to the equilibrium among steels, slag, and inclusions. This approach to inclusion control is called slag deoxidation, and it has been widely used in the production of tire-cord steels, spring steels, and low-carbon sheets [12–15]. In most slag deoxidation processes, Si is used as a deoxidizer. Zhang *et al*. [16] studied the steel–slag equilibrium with Al-killed, low-alloy steel. Because Si exhibits a lower affinity than Al for oxygen, slag deoxidation inclusions are SiO_2-containing compounds. Thus, the activity of deoxidation products can be reduced, and the activity of oxides in slag deoxidation will differ substantially from that in steel deoxidation.

In the present study, the steel–slag equilibrium in Al-killed stainless steel was investigated on the basis of industrial trials and thermodynamics calculations. VOD deoxidation refining in a 40-t EAF + VOD + ingot casting (IC) process was analyzed to deduce the mechanism of deoxidation in stainless steels and optimize the composition of the steels and slag. Moreover, methods to prevent the Al content from decreasing after deoxidation are discussed.

2. Experimental

2.1. Thermodynamics calculations

The vacuum oxygen decarburization, Al–O equilibrium, and deoxidation reaction between slag and steel were determined using the FactSage (version 6.3.1) [17] thermodynamics software. The contents of Al and Si and the slag in the deoxidation process were optimized using the software. The chemical composition of 2Cr13 stainless steel used in the calculations is shown in Table 1. The interaction coefficients employed in this study are shown in Table 2.

Table 1. Chemical composition of 2Cr13 stainless steel wt%

Al	C	Mn	Ni	P	S	Si	Cr
0.015	0.18	0.34	0.20	0.028	0.0050	0.32	12.60

Table 2. Interaction coefficients of the chemical composition in stainless steel at 1873 K [6,18]

Element	Al	C	O	Mn	Ni	P	S	Si	Cr
Al	0.043	0.091	–6.6	0.0065	–0.029	0.033	0.03	0.0056	0.0096
O	–3.9	–0.436	–0.2	–0.021	0.006	0.07	–0.133	–0.131	–0.033

2.2. Industrial trials

Industrial trials were performed to investigate the mechanism of the deoxidation process. The process of 2Cr13 stainless steel production was EAF → VOD → IC. EAF was used to melt ferrochrome and scrap with oxygen injection. The carbon content at the blowing end was 0.4wt%–0.6wt%. In the VOD process, the carbon content in the melt was further decreased by vacuum oxygen blowing. In addition, after decarburization, Al was added for deoxidation. Lime, fluxes, and fluorite were added for slagging. Ferrosilicon, silicomanganese, and ferrochrome were added to adjust the composition of the melt. Ca–Si wires were subsequently fed for inclusion modification. Ar soft blowing was performed for 10–15 min. Uphill teeming was used during ingot casting. The chemical composition of the rolled products and refining slag are shown in Table 3 and Table 4, respectively.

The total oxygen contents in the industrial trials were less than 0.003wt%. The basicity of the refining slag was controlled between 4 and 5, and the SiO_2 content varied from 8wt% to 11wt%. The acid-dissolved Al content differed among the trials.

Table 3. Chemical composition of rolled products wt%

Heat	C	Mn	Si	P	S	Cr	Als	T.O.
1	0.18	0.23	0.20	0.028	0.006	12.60	0.012	0.0027
2	0.19	0.14	0.44	0.027	0.010	13.15	0.052	0.0024
3	0.19	0.34	0.27	0.029	0.005	13.18	0.039	0.0022

Table 4. Composition of stainless steel refining slag wt%

Heat	CaO	Al_2O_3	SiO_2	MgO	Fe_2O_3	Cr_2O_3
1	51.10	23.03	11.20	5.28	0.81	0.66
2	45.19	37.20	8.52	4.55	1.14	1.32
3	59.38	21.10	10.75	6.64	0.40	0.72

2.3. Sampling and analysis method

In the industrial trials, two liquid steel samples and a final product sample were collected. Using a pail sampler (diameter 0.06 m, height 0.1 m), one liquid steel sample was

collected after deoxidation and another after Ar soft blowing. The carbon, sulfur, and total oxygen contents were measured by the infrared absorption method. Dissolved oxygen activity was determined using an oxygen probe. Other chemical compositions were measured by inductively coupled plasma atomic emission spectroscopy. The decarburization end samples were collected at temperatures from 1893 to 1973 K, whereas the deoxidation samples were collected at temperatures from 1833 to 1893 K. The composition and morphology of inclusions were analyzed by scanning electron microscopy (SEM) and energy-dispersive X-ray spectroscopy (EDS). Before teeming, the slag samples were collected and analyzed by X-ray fluorescence spectroscopy. All chemical compositions in this study are reported as mass percentage.

3. Results and discussion

3.1. Effect of vacuum decarburization on the deoxidation process in VOD

The vacuum oxygen decarburization reaction should be considered in stainless steel production. The oxygen content after the decarburization deoxidation process can be determined on the basis of the oxygen activity. However, reduction of the amount of blowing oxygen is the fundamental condition for clean stainless steel production. Applying a vacuum to the vessel removes CO, thereby allowing high Cr contents to be in equilibrium with low carbon contents. According to the literature [19] vacuum oxygen decarburization is affected by the critical carbon content, i.e., the carbon content at the end of vacuum oxygen blowing in the tank.

The effect of activity-based oxygen content on the decarburization of 2Cr13 stainless steel was calculated. During the vacuum oxygen blowing period in the VOD tank, the temperature was between 1873 and 1923 K. When the pressure was approximately 25 kPa, the top lance started to blow oxygen; the ultimate vacuum during the blow period was approximately 7–8 kPa. The result of decarburization equilibrium is shown in Fig. 1. In the VOD process, the variation of pressure in the tank affects the equilibrium to a greater extent than does the variation of temperature. Because the pressure decreases during decarburization, the equilibrium should be consistent with the results calculated for pressures between 25 kPa and 8 kPa. However, the measured data agree substantially better with the data calculated for 25 kPa. According to the studies on vacuum decarburization reported by Guo and Irons [20] and by Yamaguchi *et al*. [21], the deviation between industrial trials and the results of thermodynamics calculations is a consequence of decarburization reaction kinetics and the mass transfer of oxygen and carbon in the low oxygen and carbon range.

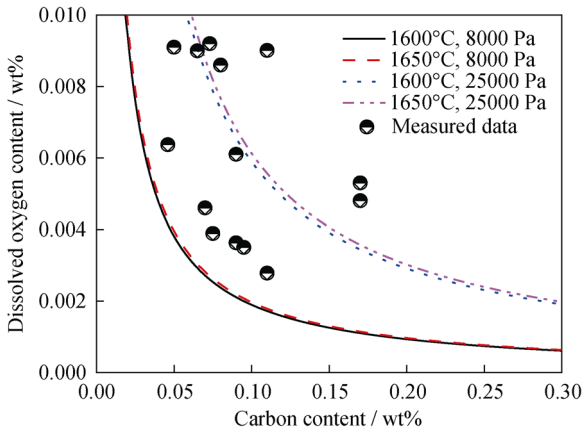

Fig. 1. Decarburization equilibrium in the 2Cr13 VOD process.

The carbon content at the end of the decarburization period in VOD was between 0.15wt% and 0.20wt%. The dissolved oxygen content in equilibrium with carbon in the melt was between 0.004wt% and 0.003wt%. If the carbon content decreases to less than 0.10wt%, the dissolved oxygen content will exceed 0.006wt%. To remove the oxygen resulting from decarburization, the amount of deoxidizer should be doubled. Therefore, the refining process in VOD is obviously affected by the vacuum decarburization, and controlling the Al content and removing Al_2O_3 from the melt are difficult when the decarburization process is unstable.

After vacuum treatment, the dissolved oxygen content was between 0.005wt% and 0.009wt%, which is much lower than the oxygen content in the process route without vacuum decarburization.

3.2. Deoxidation reaction in stainless steel

The aluminum deoxidation reaction in the VOD refining process is shown as Eq. (1). The standard Gibbs free energy of Eq. (1) is shown as Eq. (2) and Eq. (3).

$$2[\mathrm{Al}]+3[\mathrm{O}]=\mathrm{Al_2O_3(s)} \quad (1)$$

$$\Delta G^{\ominus}=-907411+235.9T \text{ [22]} \quad (2)$$

$$\Delta G^{\ominus}=-867209+222.5T \text{ [23]} \quad (3)$$

According to Eq. (1), the dissolved oxygen content is controlled by the Al content in the melt and by the Al_2O_3 activity in inclusions when the temperature is certain. In addition, if the Al_2O_3 activity is certain, the dissolved oxygen content will be governed by the Al content. The deoxidation

equilibria with different Al_2O_3 activities at 1873 K are shown in Fig. 2. 2Cr13 steel contains approximately 12.5wt%–13.5wt% Cr, which is substantially greater than the concentrations of other elements (besides iron) in the melt. In the calculations, the effect of Cr on the activity coefficients of Al and O are 0.0096 and −0.033, respectively. Thus, the Cr in melt strongly influences the activity coefficients of Al and O. The activity product of Al and O consequently decreases, and more Al must therefore be added to the stainless steel than to carbon steel to obtain the same level of dissolved oxygen.

The deoxidation equilibrium in the melt was calculated using the composition of stainless steel listed in Table 1 and the thermodynamic data provided in Table 2. As evident in Fig. 2, the lines calculated under the assumption of an Al_2O_3 activity of unity are higher than the measured values. Some of the measured values agree better with the lines calculated under an assumed Al_2O_3 activity of 0.08 or 0.03. Hence, the activity of oxygen in the refining process may be affected not only by Al but also by other reactions.

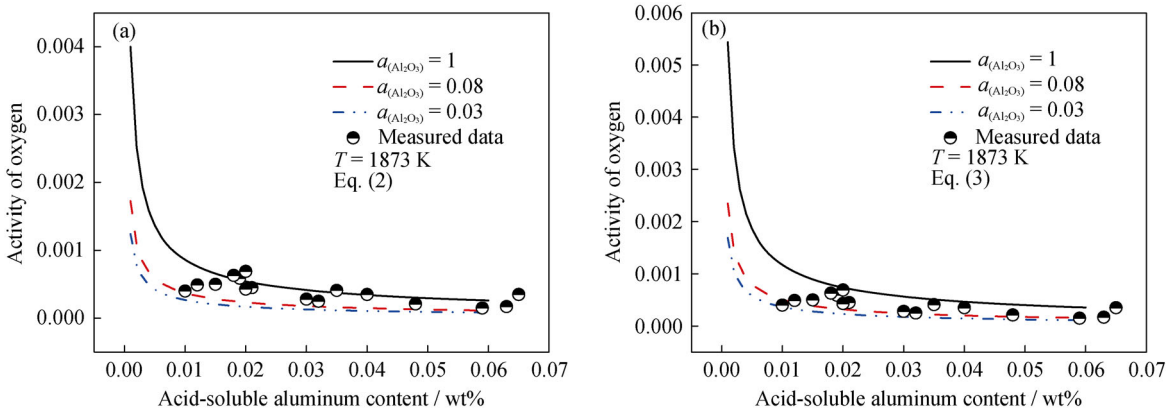

Fig. 2. Deoxidation equilibrium in 2Cr13 stainless steel.

3.3. Reduction of Cr–Mn oxides with Al in the melt

Although oxygen blowing under vacuum can remove carbon from the melt in the VOD process, some Cr and Mn in steel are still oxidized. Consequently, irregularly shaped Cr–Mn oxides are present in the melt after vacuum oxygen decarburization. During the deoxidation process, Al will reduce both dissolved oxygen as well as Cr–Mn oxides. The typical morphology and composition of the Cr–Mn oxides are shown in Fig. 3, and the reduction reactions of Cr–Mn oxides with Al are shown as follows:

$$2[Al] + Cr_2O_3(s) = Al_2O_3(s) + 2[Cr] \quad (4)$$

$$2[Al] + 3MnO(s) = Al_2O_3(s) + 3[Mn] \quad (5)$$

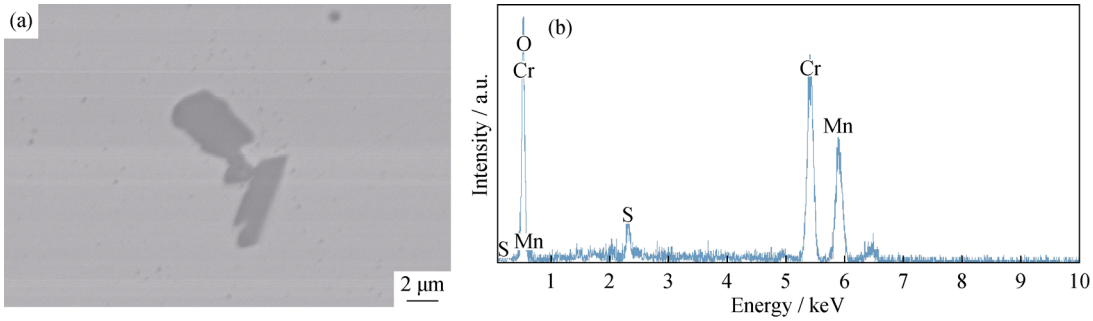

Fig. 3. SEM image (a) and EDS spectrum (b) of Cr–Mn oxides after oxygen-blowing decarburization in VOD.

The evolution of inclusions during the deoxidation process is shown in Fig. 4(a). The Cr–Mn oxides start to transform into Al–Cr oxides, and the MnO content in the inclusions will be less than 12wt% after deoxidation. The melt contains few pure Al_2O_3 inclusions, and the deoxidation products are compounds; thus, the Al_2O_3 activity will be reduced. As shown in Fig. 4(b), the Al_2O_3 activity is between 0.6 and 0.9. A decrease of the Al_2O_3 activity will drive the reaction in Eq. (1) to the right and result in a decrease in the oxygen content. However, the Al_2O_3 activity in oxides is still higher than the Al_2O_3 activity that equilibrates with liquid steel. The reduction reaction may not be the only reaction involved in deoxidation, and other reactions will occur with the Al–Cr oxides.

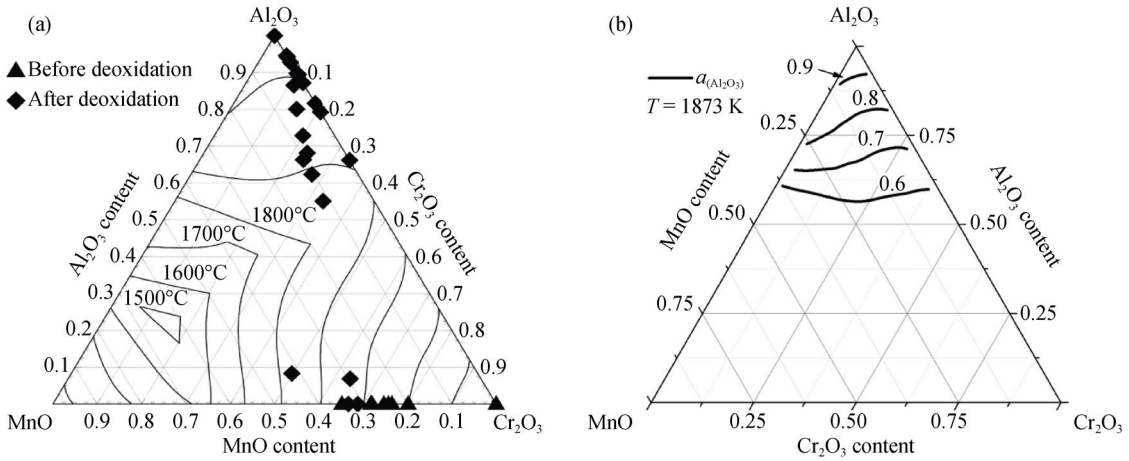

Fig. 4. Evolution of inclusions in deoxidation (a) and iso-activity lines of Al_2O_3 (b).

3.4. Deoxidation equilibrium among slag, steel, and inclusions

3.4.1. Effects of VOD refining slag on deoxidation

According to the aforementioned analysis, apart from the reduction reaction between oxides and aluminum in steel, the reaction between molten steel and refining slag can also affect the deoxidation equilibrium. First, the activities of Al_2O_3 and SiO_2 in the slag were investigated. Because the composition of the refining slag in the VOD for the manufacture of stainless steel was CaO–Al_2O_3–SiO_2–MgO, the activities of Al_2O_3 and SiO_2 were calculated in CaO–Al_2O_3–SiO_2–5wt%MgO slag by the FactSage thermodynamics software; the results are shown in Fig. 5.

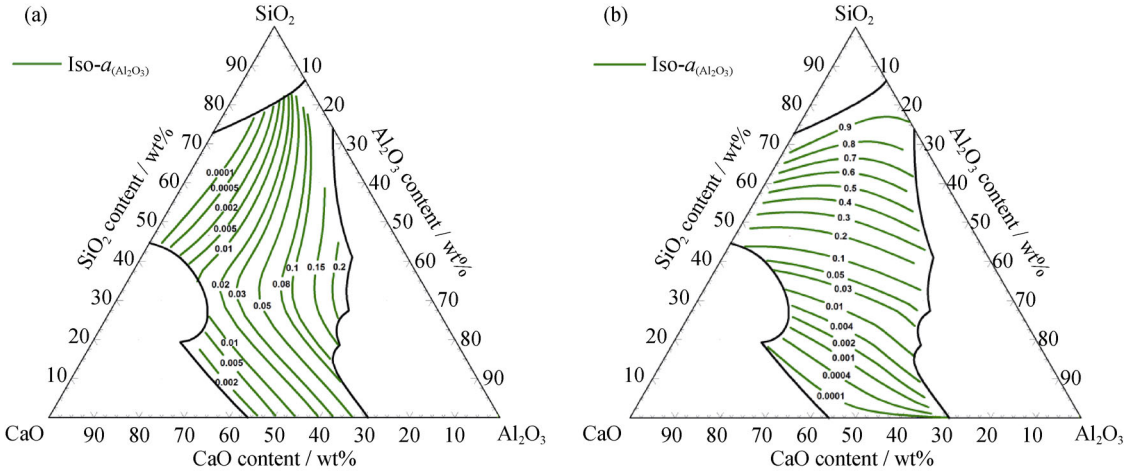

Fig. 5. Activities of Al_2O_3 (a) and SiO_2 (b) in CaO–Al_2O_3–SiO_2–5wt%MgO slag at 1873 K.

The composition of the slag substantially affects the activity of Al_2O_3 in the slag. When the content of SiO_2 is less than 40wt%, the activity of Al_2O_3 is governed by the content of CaO; thus, an increase in the amount of CaO can diminish the activity of Al_2O_3. When the SiO_2 content is greater than 40wt%, the activity of Al_2O_3 is related to the SiO_2 content in the slag. As shown in Fig. 6, when the basicity (w(CaO)/w(SiO_2)) exceeds 3, the activity of Al_2O_3 is relatively small and remains constant with a change in basicity. A high basicity of the slag facilitates the Al–O reaction between the slag and the steel, thereby reducing the dissolved oxygen content in the molten steel.

The activity of SiO_2 decreases with decreasing SiO_2 content. When the SiO_2 content is less than 40wt%, the activity of SiO_2 is affected by CaO and decreases with increasing CaO content. On the basis of the composition of the slag listed in Table 4, the activity of Al_2O_3 is less than 0.008. By contrast, according to the Al–O trial data in Fig. 2, the activity of Al_2O_3 in the deoxidation product is approximately equal to that in the refining slag. After deoxidation and slagging in VOD, strong stirring during the degassing process of VOD provides excellent dynamic conditions for the slag–steel reaction and can further contribute to this reaction. Therefore, the slag–steel reaction can reach an equilibrium

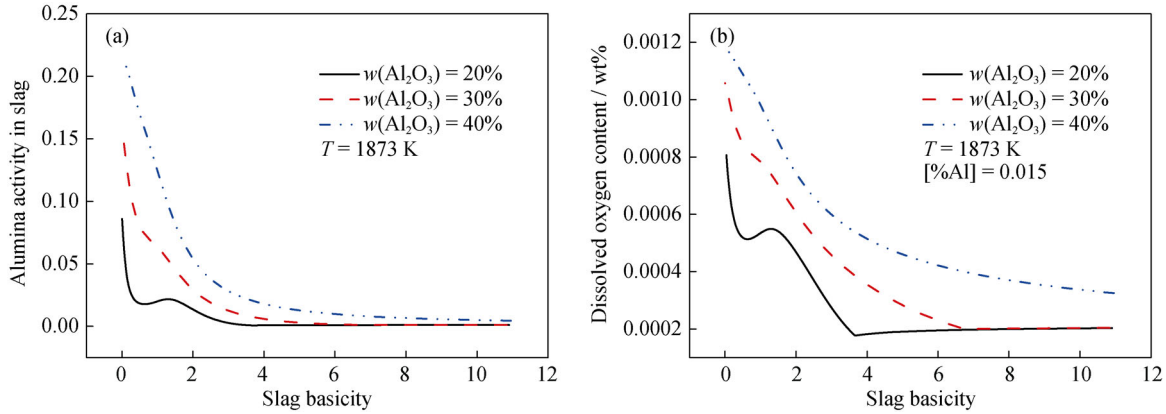

Fig. 6. Influence of slag basicity on Al_2O_3 activity (a) and dissolved oxygen content (b).

state in the VOD refining process.

According to the aforementioned analysis, the deoxidation mechanism is slag deoxidation, which differs from the deoxidation mechanism in the refining of cord steel as well as those in the refining of other steel grades using a ladle furnace (LF) and RH treatment [24]. In the VOD refining process of stainless steel, excellent steel–slag reaction conditions are obtained by strong stirring under vacuum conditions, which can reduce the activity of deoxidation products in a state of reaction equilibrium and reduce the dissolved oxygen content in the stainless steel. When the basicity of the refining slag ranges from 3 to 5, the activity of Al_2O_3 can be controlled to be less than 0.008, where it remains stable, and the dissolved oxygen content can be controlled to be less than 0.0006wt%.

3.4.2. Control of Al–Si via equilibrium of the steel–slag reaction

In the deoxidation of stainless steel and slag, the primary deoxidants are Al and Si, which react with FeO and MnO in the slag. Because of the strong oxidizability of FeO and MnO, Al powder can react with them rapidly, thereby decreasing the oxidizability of the slag. According to the work of Todoroki and Mizuno [4] on the refining slag of stainless steel, the presence of SiO_2 in the slag can affect the deoxidation reactions in molten steel and is a source of oxygen in the melting process of stainless steel. To avoid a decrease in the amount of acid-soluble Al as a consequence of reduction of SiO_2 in slag during the refining process, the Al–Si equilibrium of slag–steel was calculated. The Al–Si equilibrium reaction is shown in Eq. (6) [14].

$$4[\mathrm{Al}] + 3(\mathrm{SiO_2}) = 2(\mathrm{Al_2O_3}) + 3[\mathrm{Si}] \tag{6}$$

$$\Delta G^{\ominus} = -658300 + 107.2T, \text{ J/mol} \tag{7}$$

On the basis of Eq. (6) and the activity of Al_2O_3 and SiO_2 in the refining slag, the iso-[%Si] lines were obtained, as is shown in Fig. 7. A comparison of the iso-Si lines for different Al contents reveals that the iso-Si lines decrease slightly as the Al content is increased from 0.015wt% to 0.05wt%. Therefore, decreasing the SiO_2 content by enhancing the Al content in steel is difficult because the Si content in stainless steel tends to be constant. Because of the Si–O equilibrium between the steel and slag, enhancing the Si content in molten steel will increase the SiO_2 content in the slag, particularly when the SiO_2 content is less than 5wt%. As a result, the Si content in molten steel should be reduced in the VOD slagging process so that a high-basicity slag can be formed. After slagging and deoxidation in the VOD process, the composition of the slag changes slightly. According to the equilibrium constant for Eq. (6), which is shown as follows:

$$K = \frac{a_{[\mathrm{Si}]}^3 a_{(\mathrm{Al_2O_3})}^2}{a_{[\mathrm{Al}]}^4 a_{(\mathrm{SiO_2})}^3} \tag{8}$$

Al–Si equilibrium in molten steel can be achieved when the activities of Al_2O_3 and SiO_2 are constant.

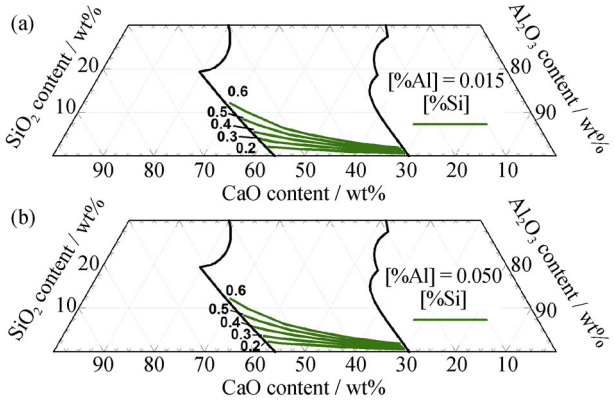

Fig. 7. Iso-[%Si] lines in equilibrated slag–steel with different Al contents.

The relationship between $a_{(\mathrm{Al_2O_3})}^2 / a_{(\mathrm{SiO_2})}^3$ in the slag and the basicity of the slag is shown in Fig. 8(a). When the basicity of the slag is greater than 3, the $a_{(\mathrm{Al_2O_3})}^2 / a_{(\mathrm{SiO_2})}^3$ ratio

in the slag is relatively large and tends to fluctuate only slightly with changes in the basicity. Figs. 8(b), 8(c), and 8(d) represent the Al–Si equilibrium in molten steel according to the calculated slag activities. As shown in the figure, to increase the acid-dissolved Al beyond 0.015wt%, the Si content in the steel should be greater than 0.5wt%. Furthermore, decreasing the Al_2O_3 content in the slag and increasing the basicity of the slag are beneficial to maintaining the content of acid-dissolved Al after deoxidation. In VOD, Al is used in the deoxidation process; thus, controlling the Si content within the required range is difficult. The Al content is mostly governed to be between 0.02wt% and 0.05wt%; therefore, the content of acid-dissolved Al decreases in the final stage of the refining process, which can result in a gentle decrease or even an increase in the total oxygen during the soft-blowing process in VOD.

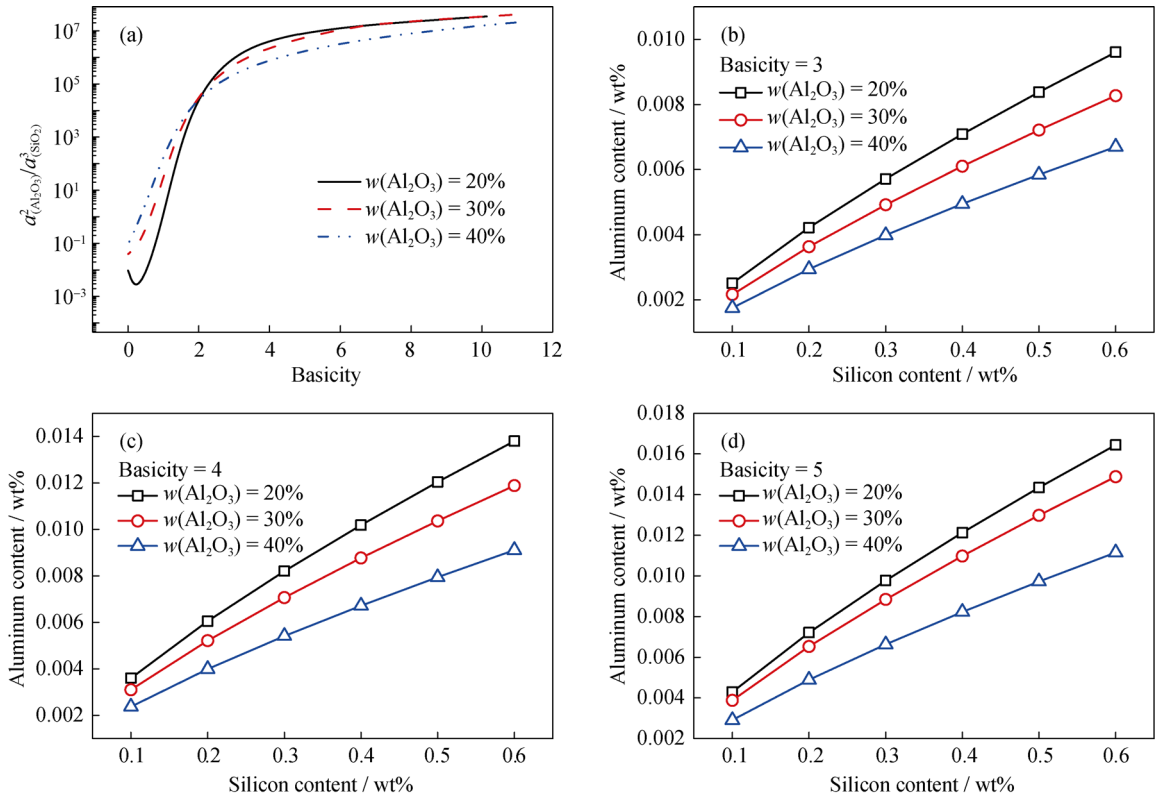

Fig. 8. Influence of slag basicity on the activity of oxides (a) and on the Al–Si equilibrium in steel–slag (b–d).

The basicity of slag can be controlled above 5 when the SiO_2 content in the slag is 10wt% or 5wt%. However, from the perspective of industrial production, reduction of SiO_2 in the slag will increase the cost and difficulty. Thus, to reduce Al consumption, both the basicity of the slag and the effect of SiO_2 content on the reaction should be investigated. As shown in Fig. 9, the SiO_2 activity is substantially affected when the SiO_2 content is less than 2.5wt%. Otherwise, SiO_2

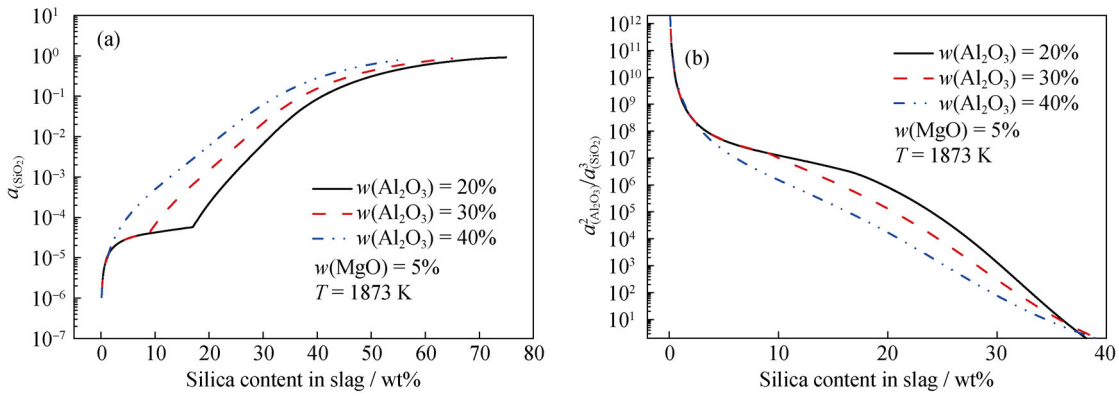

Fig. 9. Effect of SiO_2 content on the activity of SiO_2 (a) and oxides (b).

activity is controlled by Al_2O_3 and SiO_2 in the slag. To obtain a low level of SiO_2 activity, the SiO_2 content should be reduced and the Al_2O_3 content should be increased.

The effect of SiO_2 content on dissolved Al in steel was calculated; the results are shown in Fig. 10. As evident in the figure, the Al_2O_3 content clearly affects the reaction of Al and SiO_2. Therefore, the Al_2O_3 content should be in the range from 20wt% to 30wt%. When the Al content is assured as 0.015wt% in the melt, the SiO_2 content equilibrated with Si contents of 0.3wt% and 0.4wt% should be 5wt% and 8wt%, respectively.

In summary, the excellent dynamic conditions in VOD contribute to the deoxidation of stainless steel. When the basicity of the slag is between 3 and 5, the oxygen activity is relatively low. In the slagging process, a high basicity and a low SiO_2 content in the slag can be achieved by reducing the Si content in the molten steel. The decrease of acid-dissolved Al generated by reduction of SiO_2 can be avoided when a slag with high basicity and a low Al_2O_3 content is utilized, as well as Si content in melt is enhanced in subsequent refining processes.

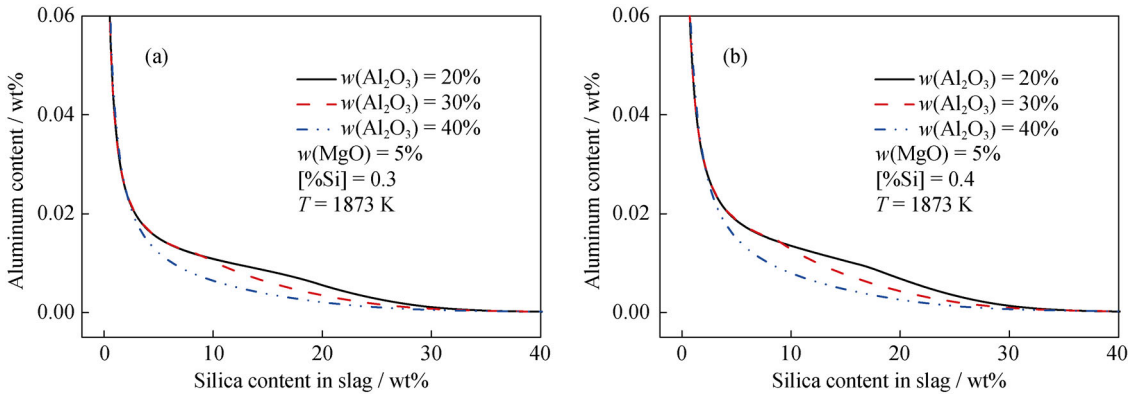

Fig. 10. Effect of SiO_2 content on dissolved Al in steel.

4. Conclusion

(1) The vacuum decarburization reaction reduced the dissolved oxygen content in stainless steel. Controlling the Al content and removing Al_2O_3 from the melt were difficult in the absence of a stable decarburization process.

(2) The deoxidation process of stainless steel includes the following reactions: the deoxidation reaction in liquid steel, the reduction of Cr–Mn oxides by reaction with Al in the melt, and deoxidation equilibrium among the slag, steel, and inclusions.

(3) The fine stirring conditions during the deoxidation process leading to equilibrium among the steel, slag, and inclusions and the oxygen activity were controlled by the slag and by the Al in the melt. A basicity between 3 and 5 and an Al content greater than 0.015wt% in the melt resulted in an oxygen content less than 0.0006wt%. The dissolved oxygen content decreased slightly when the Al content in the steel exceeded 0.02wt%.

(4) Because of the equilibrium of the Si–O reaction between the slag and steel, the activity of SiO_2 in the slag will increase with increasing Si content. Accordingly, to form a high-basicity slag, the Si content should be decreased in the steel before slagging. A high-basicity and low-Al_2O_3-content slag with an elevated Si content after slagging will reduce the Al consumption caused by SiO_2 reduction.

Acknowledgements

This work was financially supported by the China Postdoctoral Science Foundation (Nos. 2015T80039 and 2014M560890). The authors thank the engineers at the Technology Center and the No. 2 Steelmaking Plant of Changcheng Special Steel for their assistance with industrial trials.

References

[1] D.H. Mesa, A. Toro, A. Sinatora, and A.P. Tschiptschin, The effect of testing temperature on corrosion–erosion resistance of martensitic stainless steels, *Wear*, 255(2003), No. 1-6, p. 139.

[2] Z.Y. Yang, Z.B. Liu, J.X. Liang, Y.Q. Sun, and W.H. Li, Development of maraging stainless steel, *Trans. Mater. Heat Treat.*, 29(2008), No. 4, p. 1.

[3] H. Ohta and H. Suito, Thermodynamics of aluminum and manganese deoxidation equilibria in Fe–Ni and Fe–Cr alloys, *ISIJ Int.*, 43(2003), No. 9, p. 1301.

[4] H. Todoroki and K. Mizuno, Effect of silica in slag on inclusion compositions in 304 stainless steel, deoxidized with aluminum, *ISIJ Int.*, 44(2004), No. 8, p. 1350.

[5] W.Y. Cha, D.S. Kim, Y.D. Lee, and J.J. Pak, A thermody-

namic study on the inclusion formation in ferritic stainless steel melt, *ISIJ Int.*, 44(2004), No. 7, p. 1134.

[6] J.H. Park, Thermodynamic investigation on the formation of inclusions containing $MgAl_2O_4$ spinel during 16Cr–14Ni austenitic stainless steel manufacturing processes, *Mater. Sci. Eng. A*, 472(2008), No. 1-2, p. 43.

[7] J.W. Kim, S.K. Kim, D.S. Kim, Y.D. Lee, and P.K. Yang, Formation mechanism of Ca–Si–Al–Mg–Ti–O inclusions in type 304 stainless steel, *ISIJ Int.*, 36(1996), Suppl., p. S140.

[8] Y.H. Sun, Y.N. Zeng, R. Xu, and K.K. Cai, Formation mechanism and control of $MgO{\cdot}Al_2O_3$ inclusions in non-oriented silicon steel, *Int. J. Miner. Metall. Mater.*, 21(2014), No. 11, p. 1068.

[9] Z.Y. Deng and M.Y. Zhu, Evolution mechanism of non-metallic inclusions in Al-killed alloyed steel during secondary refining process, *ISIJ Int.*, 53(2013), No. 3, p. 450.

[10] K. Suzuki, S. Ban-Ya, and M. Hino, Deoxidation equilibrium of Cr–Ni stainless steel with Si at the temperatures from 1823 to 1923 K, *ISIJ Int.*, 42(2002), No. 2, p. 146.

[11] S.B. Lee, J.H. Choi, H.G. Lee, P.C. Rhee, and S.M. Jung, Aluminum deoxidation equilibrium in liquid Fe–16 pct Cr alloy, *Metall. Mater. Trans. B*, 36(2005), No. 3, p. 414.

[12] H. Suito and R. Inoue, Thermodynamics on control of inclusions composition in ultra-clean steels, *ISIJ Int.*, 36(1996), No. 5, p. 528.

[13] S. Nurmi, S. Louhenkilpi, and L. Holappa, Optimization of intensified silicon deoxidation, *Steel Res. Int.*, 84(2013), No. 4, p. 323.

[14] H. Ohta and H. Suito, Activities in $CaO–SiO_2–Al_2O_3$ slags and deoxidation equilibria of Si and Al, *Metall. Mater. Trans. B*, 27(1996), No. 6, p. 943.

[15] X.H. Wang, M. Jiang, B. Chen, and H.B. Li, Study on formation of non-metallic inclusions with lower melting temperatures in extra low oxygen special steels, *Sci. China Technol. Sci.*, 55(2012), No. 7, p. 1863.

[16] J. Zhang, F.M. Wang, and C.R. Li, Thermodynamic analysis of the compositional control of inclusions in cutting-wire steel, *Int. J. Miner. Metall. Mater.*, 21(2014), No. 7, p. 647.

[17] FactSage: http://www.factsage.com.

[18] G.K. Sigworth and J.F. Elliott, The thermodynamics of liquid dilute iron alloys, *Met. Sci.*, 8(1974), No. 1, p. 298.

[19] G.P. Wang, Z.B. Li, and C.L. Liu, Effect of VOD & LF processes on stainless steel cleanliness, [in] *The 7th CSM Steel Congress*, Beijing, 2009, p. 1262.

[20] D. Guo and G.A. Irons, Modeling of gas-liquid reactions in ladle metallurgy: Part I. Physical modeling, *Metall. Mater. Trans. B*, 31(2000), No. 6, p. 1447.

[21] K. Yamaguchi, Y. Kishimoto, T. Sakuraya, T. Fujii, M. Aratani, and H. Nishikawa, Effect of refining conditions for ultra low carbon steel on decarburization reaction in RH degasser., *ISIJ Int.*, 32(1992), No. 1, p. 126.

[22] J.D. Seo, S.H. Kim, and K.R. Lee, Thermodynamic assessment of the Al deoxidation reaction in liquid iron, *Steel Res. Int*, 69(1998), No. 2, p. 49.

[23] H. Itoh, M. Hino, and S. Ban-Ya, Assessment of Al deoxidation equilibrium in liquid iron, *Tetsu-to-Hagane*, 83(1997), No. 12, p. 773.

[24] Z.Y. Deng and M.Y. Zhu, Deoxidation mechanism of Al-killed steel during industrial refining process, *ISIJ Int.*, 54(2014), No. 7, p. 1498.